

Compatibility Study in Poly(tetramethyleneadipate-co-terephthalate)/Polystyrene Bioblends

Girma Biresaw,¹ Abdellatif Mohamed,¹ Sherald H. Gordon,¹ Rogers E. Harry-O'kuru,² Craig C. Carriere³

¹Cereal Products and Food Science Research Unit, National Center for Agricultural Utilization Research, Agricultural Research Service, United States Department of Agriculture, Peoria, Illinois 61604

²New Crops and Products Research Unit, National Center for Agricultural Utilization Research, Agricultural Research Service, United States Department of Agriculture, Peoria, Illinois 61604

³CoBatco Inc., 1215 North East Adams Street, Peoria, Illinois 61550

Received 7 April 2008; accepted 27 June 2008

DOI 10.1002/app.28893

Published online 2 September 2008 in Wiley InterScience (www.interscience.wiley.com).

ABSTRACT: Bioblends of the biodegradable copolyester poly(tetramethyleneadipate-co-terephthalate) (EBU) and polystyrene (PS) were prepared in different weight compositions on a twin-screw extruder at 160–200°C. The various blend compositions were then investigated using thermogravimetric analysis (TGA), modulated differential scanning calorimetry (MDSC), and Fourier transform infrared photoacoustic spectroscopy (FTIR-PAS). TGA studies showed that 25/75 and 50/50 EBU/PS blends had higher thermal stability than the more thermally stable blend component, PS. The MDSC studies showed a single T_g and single T_m for the blends, that were concentration independent. The FTIR-PAS studies indicated a small shift (4–8

cm^{-1}) in the carbonyl absorption peaks of EBU to lower wavenumbers in 50/50 EBU/PS blend relative to that of neat EBU. It is concluded that, while the MDSC results were inconclusive, the TGA and FTIR-PAS results support the existence of some degree of intermolecular interaction between EBU and PS components and, hence, partial compatibility in EBU/PS blends. © 2008 Wiley Periodicals, Inc. *J Appl Polym Sci* 110: 2932–2941, 2008

Key words: poly(tetramethyleneadipate-co-terephthalate); polystyrene; bioblends; TGA; MDSC; FTIR-PAS; polymer blend compatibility; degradation kinetics; degradation activation energy

INTRODUCTION

Biodegradable polymers are synthetic polymers that have excellent water-resistance properties (like most synthetic polymers), while at the same time being biodegradable (like most natural polymers). This unique combination of properties makes biodegradable polymers ideal ingredients in the development of a variety of products for use in manufacturing, household, medical, and other applications. Biodegradable polymers are obtained from chemical and/or enzymatic synthesis of a variety of precursors, including those from agriculture-based renewable sources such as corn. Examples of biodegradable polymers include polylactic acid (PLA), polycaprolactone (PCL), and poly(hydroxybutyrate-co-hydroxyvalerate) (PHBV).¹

Names are necessary to report factually on available data; however, the USDA neither guarantees nor warrants the standard of the product, and the use of the name by the USDA implies no approval of the product to the exclusion of others that may also be suitable.

Correspondence to: G. Biresaw (girma.biresaw@ars.usda.gov).

Biodegradable polymers are blended with each other, and with other natural and synthetic polymers in the development of materials that are fully or partially biodegradable.^{2–17} Polymer blends containing at least one biodegradable polymer component are referred to as bioblends. Natural polymers such as gluten,¹⁸ starch,^{5,7,13,15,16,19,20} and lignin¹³ have been blended with biodegradable polymers and investigated using a variety of methods. Such investigations have been conducted with and without the application of different types of compatibilizers, plasticizers, and salts.²¹

Products under active development from bioblends include those for: (a) materials/packaging applications; (b) drug delivery systems, i.e., encapsulation and controlled release of drugs from a variety of implantable and nonimplantable formulations; and (c) cell culture/tissue engineering applications such as bioabsorbable sutures and tissue transplantation.²²

Development of useful products from bioblends requires that the polymers be compatible with each other. Compatibility is a function of the physical and chemical properties of the polymers being blended, as well as the blending parameters (e.g., temperature, pressure, humidity, shear, etc.).^{23–26} Currently, there are a variety of methods that are being used to

assess the degree of compatibility of blends. These methods can be broadly categorized into: interfacial, thermal, mechanical, morphological, spectroscopic, and scattering techniques.^{23–26} However, there are no quantitative models for predicting blend compatibility from component properties and/or blending parameters. This lack of knowledge has impeded the rapid development of useful products from bio-blends.

To increase our understanding of compatibility in blends comprising biodegradable polymers, our group initiated studies on model bioblends. These are binary blends in which one component is a biodegradable polymer and the second component is the nonbiodegradable polymer polystyrene (PS). In previous studies, we examined the properties of the model bioblends using a variety of methods such as interfacial tension,^{27–29} interfacial adhesion,³⁰ tensile,³¹ rheological,³² and morphological³² measurements.

In the work described here, we extend our investigation into compatibility of bioblends using thermogravimetric analysis (TGA), differential scanning calorimetry (DSC), and Fourier transform infrared/photoacoustic spectroscopy (FTIR-PAS) methods. The bioblend investigated is comprised of PS and the biodegradable polymer Poly(tetramethyleneadipate-*co*-terephthalate) also known under the trade name Eastar Bio Ultra[®] or EBU. EBU was selected because it is a commercially available biodegradable polymer, and also because of the current intense interest in developing biomaterials from EBU blends. The ultimate goal of this investigation is that of developing improved understanding of compatibility, and the development of compatibility predictive models applicable to blends with biodegradable polymers.

EXPERIMENTAL

Materials

Polymers investigated in this work were obtained from commercial sources and were used as received. Poly(tetramethyleneadipate-*co*-terephthalate) (Eastar Bio Ultra or EBU) was obtained from Eastman (Eastman Chemical Resins, West Elizabeth, PA); and PS from Dow Chemical Co. (trade name: Styron 685D).

Polymer blend preparation

Binary blends of EBU with PS were prepared by manually mixing the corresponding pellets followed by extrusion into ribbons on a ZSK-30 twin-screw extruder (Werner and Pfleiderer, Ramsey, NJ). The extrusion conditions were: extrusion temperature (zones no. 1 through no. 7), 77–200°C; rotor speed,

151–200 rpm; residence time, 3–5 min. The ribbons exiting the extruder were fed into a Bronco II mechanical chopper (Killion, Cedar Grove, NJ), which converted the ribbons into pellets. Some of the blends required more time to solidify and were cut into pellets manually after the extrusion was completed. The composition of the EBU/PS blends were (% w/w): 100/0, 85/15, 75/25, 50/50, 35/65, 25/75, 0/100. Details of the extrusion procedure are given elsewhere.³¹

Property evaluation

The binary blends of EBU with PS and the two neat polymers (EBU and PS) were characterized using the following methods.

Thermogravimetric analysis

TGA analysis was done using a TGA 2050 Thermogravimetric Analyzer (TA Instruments, New Castle, DE). Samples were ground into powder using a Brinkmann/Retsch high-speed shaker mill. Samples (~ 10 mg) were heated from 25 to 800°C at 10°C/min and held at an isotherm for 3 min. The TGA data were plotted as temperature versus weight %, from which onset, peak, and final decomposition temperatures were obtained (hereafter, these plots will be referred to as TGA plots). The TGA data were also plotted as temperature versus derivative of weight residue %, from which peak decomposition temperatures were obtained (these plots will be referred to as DTGA plots).

Modulated differential scanning calorimetry

Modulated differential scanning calorimetry (MDSC) measurements were performed using a TA Modulated DSC[™] 2920 (TA Instruments, New Castle, DE). As with TGA, powdered sample (~ 50 mg) was loaded in a stainless steel pan and the pan was then sealed. Once loaded on the MDSC, the sample was equilibrated at 0°C, after which the temperature increased at 10°C/min to 200°C; an isotherm was maintained for 1 min; then, the sample was cooled at 10°C/min to –70°C. This process was repeated for each blend, for up to 200 cycles.

Fourier transform infrared photoacoustic spectroscopy

Three different binary blends of EBU with PS and the two neat polymers (EBU and PS) were tested by FTIR-PAS. Samples were tested in the solid state as received with no pulverization, treatment or other sample preparation. Each pellet (~ 3 mm thick) was

placed in FTIR-PAS detector (MTEC PAS cell, Model 200, MTEC, Ames, IA) and purged with helium for ~ 15 min to maximize the photoacoustic signal-to-noise ratio. Samples were equilibrated in the PAS cell at 25°C before testing. FTIR-PAS spectra were measured using the MTEC detector on an FTS 6000 spectrometer (Varian, Walnut Creek, CA) equipped with a KBr crystal beamsplitter. The light source was a water-cooled ceramic mid-infrared globar delivering 150 mW energy to the sample compartment. Step-scan phase modulation at 400 Hz and 2.0 $\lambda_{\text{He-Ne}}$ amplitude was applied at a step rate of 2.5 Hz with software-based digital signal processing (DSP) supplied with the Win-IR-Pro software provided by Varian. For the polymers in this study, the 400 Hz modulation frequency probed a sampling depth of ~ 9 μm into the pellet. PAS spectra were acquired from symmetric interferograms by correcting the phase rotation angle and ratioing of the signals against a carbon black reference. DSP generated in-phase (0°) and quadrature (90°) components of the PAS signals. The photoacoustic signals were collected and averaged over two 1024 point scans. Interferograms were Fourier transformed using triangular apodization for optimum linear response.

Depth-specific phase angle spectra of the polymers were computed by 3D interpolation as the root-mean-square values of the 0° and 90° components. Spectra were truncated to isolate the EBU carbonyl region ($1850\text{--}1650\text{ cm}^{-1}$) and plotted for subsequent resolution and graphical visualization. 3D interpolation spectra were normalized to the phase angle at which the photoacoustic response is maximized prior to spectral deconvolution of the carbonyl band.

Resolution and graphical visualization of FTIR-PAS spectra

Overlapping carbonyl bands in neat EBU and EBU/PS blends were resolved and visualized using routines provided in IR spectral software, GRAMS AI, supplied by Thermo Galactic, (Salem, NH). Separation of the individual carbonyl peaks was enhanced by Fourier self-deconvolution using a Lorentzian band shape with a Bessel smoothing function. The number of overlapping peaks and their locations were automatically determined by a second derivative algorithm in the software. The determined number of peaks were recursively fitted to the measured carbonyl band, which exhibited pronounced asymmetry, using combination Gaussian/Lorentzian band shapes. The two salient Gaussian/Lorentzian peaks which overlapped were truncated and digitally joined at their intersections. The resulting doublet peak shapes were scaled for visualization in

plots to best contrast the measured carbonyl bands in neat EBU with EBU/PS blends.

RESULTS AND DISCUSSION

Thermogravimetric analysis

TGA is used to evaluate the thermal stability of polymers and blends.³³ The higher the decomposition temperature, the more stable the polymer or blend. Blending could have a negative (destabilizing) or positive (stabilizing) effect on thermal stability. Thus, the thermal stability of blends is evaluated relative to that of its components. Such evaluation along with other data are used to infer various blend characteristics such as interaction and miscibility of the polymers in the blend.

In general, the effect of blending on thermal stability can be grouped into one of the following three categories: (a) The thermal stability of the blend is higher than that of the more stable blend component.^{34,35} Such observations are interpreted as a definite improvement in thermal stability due to blending. It is sometimes considered as corroborating evidence for the existence of strong interaction between polymers in the blend, which could lead to miscibility (b) The thermal stability of the blend is lower than the least stable component.^{36–39} Such observations are an indication of worsening of thermal stability due to blending. It is considered as corroborating evidence for the absence of any fruitful interaction between blend components. In many instances, such an outcome is considered as corroborating evidence for a phase-separated, and immiscible, blend. (c) The thermal stability of the blend is intermediate between those of the components.^{40–47} This observation could imply an improvement, worsening, or no change in the thermal stability as a result of blending. Such observations have been interpreted as an improvement in the thermal stability of one component or worsening of thermal stability of another component. Careful analysis of the TGA data is required to properly interpret such TGA outcomes. In situations where improvement in thermal stability has been indicated, such an outcome has been interpreted as corroborating evidence for some degree of intermolecular interaction between blend components.

Figure 1 shows the TGA and DTGA of EBU/PS blends. As can be seen in Figure 1, both neat polymers displayed a simple decomposition profile with a single transition temperature. The data also show that the neat biodegradable polyester EBU has a lower thermal stability than PS. Also, EBU displayed a char residue of 6% (w/w) at 440°C, which decreased gradually to 3.5% (w/w) at 800°C. On the other hand no char residues were displayed by PS.

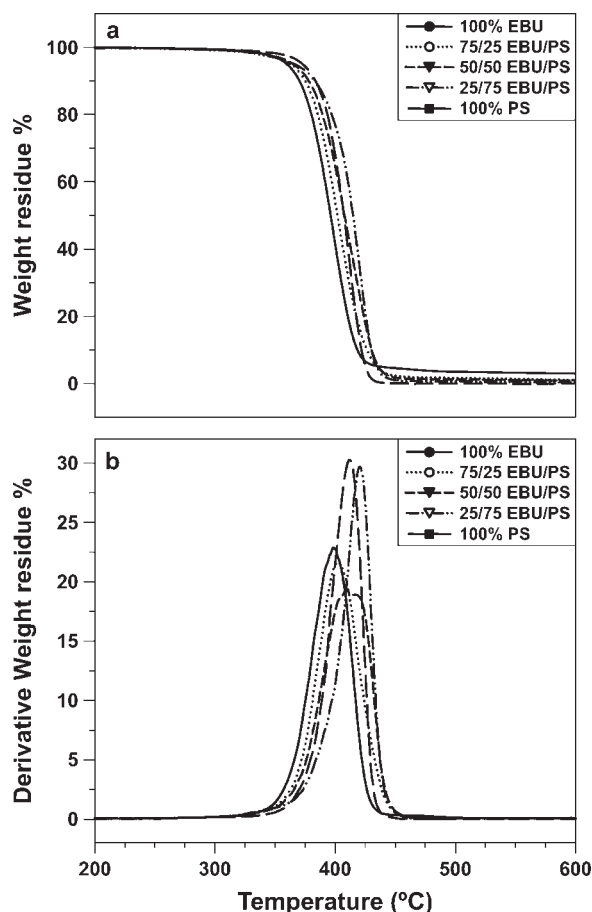


Figure 1 TGA (a) and DTGA (b) profiles of EBU/PS bioblends.

The onset, final, and peak thermal degradation temperatures of the neat polymers and blends are summarized in Table I.

Examination of the TGA profiles of EBU/PS blends shows a single transition temperature at all blend compositions. The blends also displayed no char residues even at high EBU composition. This implies that PS might be catalyzing complete thermal decomposition of the biodegradable polyester. The onset, final and peak values of the decomposi-

TABLE I
Onset, Peak, and Final Decomposition Temperatures (°C) from TGA and DTGA Analysis of EBU, PS and EBU/PS Blends

Sample	Onset	Peak ^a	Final
100% EBU	383.3	407.0	424.7
75/25 EBU/PS	385.8	404.4	429.4
50/50 EBU/PS	388.7	414.6	436.5
25/75 EBU/PS	406.0	428.3	440.0
100% PS	398.4	418.5	430.4

^a Peak temperature corresponds to the temperature of maximum rate of decomposition, obtained from DTGA plots such as that shown in Figure 1(b).

tion temperatures varied with blend compositions. As shown in Table I, for some EBU/PS blend compositions, these values were between those of neat EBU and neat PS. However, for EBU/PS blend of 50/50, the final decomposition temperature was higher than those of neat PS, which is the more thermally stable of the two blend components. Also, the onset, peak and final decomposition temperatures for 25/75 EBU/PS blend were higher than those for neat PS.

Degradation kinetics

TGA was also used to determine the degradation kinetics of neat EBU, neat PS and EBU/PS blends. Three heating rates, 10, 15, and 20°C/min, were used to calculate the activation energy of degradation (E_a) according to the Flynn and Wall equation⁴⁸

$$\log \beta = 0.457 \left(-\frac{E_a}{RT} \right) + \left[\log \left(\frac{AE_a}{R} \right) - \log F(a) - 2.315 \right] \quad (1)$$

where β is the heating rate in °C/min, T is the absolute temperature in K, R is the universal gas constant, a is the percent conversion, E_a is the activation energy, and A is the pre-exponential factor.

According to eq. (1), at a constant conversion, E_a can be obtained from the slope of the plot of $1000/T$ (K) versus $\log \beta$. Software provided with the instrument by TA Instruments is used to automatically calculate E_a . E_a values were determined for all samples and percent conversions. Figure 2 shows the percent conversion plotted against E_a of degradation. The shape of the percent conversion versus E_a curve can be used to infer the mechanism of degradation of the sample. In general, when this relationship is linear it signifies a one-step degradation mechanism,

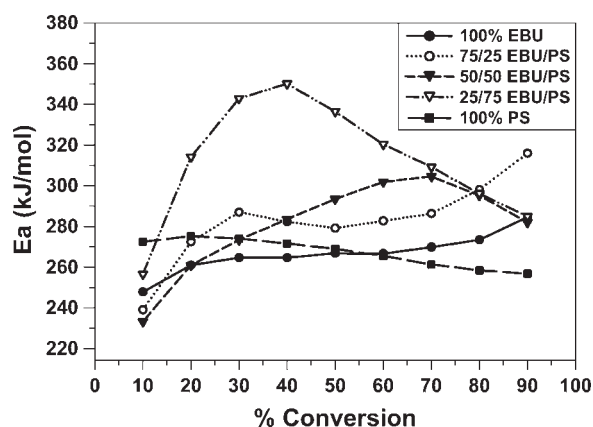


Figure 2 Activation energy of degradation (E_a) versus percent conversion of EBU/PS blends from analysis of TGA data using the Flynn-Wall-Ozawa method.

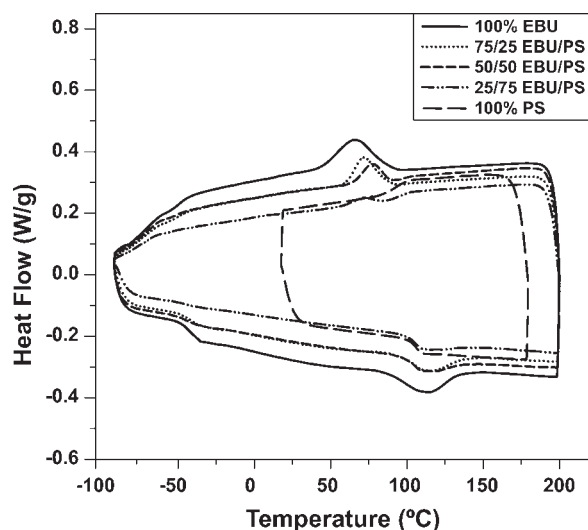


Figure 3 MDSC profile of EBU/PS bioblends.

whereas a nonlinear relationship is an indication of a multistep degradation process. The data in Figure 2 show a linear relationship for the neat polymers (EBU and PS), which is an indication of a one-step degradation process. On the other hand, the blends gave a nonlinear relationship, which is an indication of a two or three-step degradation mechanism.

Modulated differential scanning calorimetry

DSC allows the determination of transition temperatures (T_g , T_m , T_c) and associated heat flows (ΔH_f , ΔH_c , ΔC_p) of polymers.²⁴ Neat polymers have characteristic DSC profiles that depend on the nature of the polymer. Amorphous polymers display characteristic T_g , crystalline polymers display characteristic T_m , and semicrystalline polymers display both T_g and T_m .

DSC properties of polymers can be affected when they are blended with other materials (e.g., other polymers, plasticizers, compatibilizers, etc.). The changes in DSC properties of blends might be due to intermolecular interactions between the polymers in the blend. As a result, DSC can be used to obtain qualitative and quantitative information about various blend characteristics by analyzing the effect of blend composition on the transition temperatures and heat flows. Blend characteristics that can be predicted based on DSC measurements include: degree of miscibility,^{49–51} degree of intermolecular interactions,^{33,52,53} degree of crystallization.^{51,54,55} The general rule for evaluating miscibility of binary blends using DSC is as follows: (a) immiscible – blends that display two T_g s and two T_m s that are composition-independent^{46,51,56}; (b) miscible – blends that display composition-dependent single T_g and single T_m in the entire composition range,^{33,46,50} (c) partially miscible – blends that display two T_g s and two T_m s that are composition dependent,^{42,49,57} and/or composition-dependent single T_g and single T_m in a narrow composition range.

The DSC of EBU/PS blends are compared in Figure 3. The DSC data are from the second cycle of a 200 cycle DSC run. As can be seen in Figure 3, neat PS displayed a single peak corresponding to its characteristic T_g (103–110°C). Neat EBU displayed three peaks: T_g around -39°C , T_c (crystallization) around 67°C , and T_m (melting) around 115°C . The data in Table II show that the measured T_m and T_g values of the neat polymers were within the range reported by the manufacturers.

EBU/PS blends displayed three peaks which were determined to be the T_g , T_c , and T_m values close to those of neat EBU. Table II summarizes the onset (T_o), peak (T_p), midpoint (T_{mid}), and final (T_f) values of the transition temperatures. Also shown in Table

TABLE II
Summary of MDSC Data on EBU, PS, and EBU/PS Blends^a

Sample	Melting (T_m) ^b			Crystallization (T_c) ^b			Glass Transition (T_g) ^c			
	T_o	T_p	ΔH_m ^d	T_o	T_p	ΔH_c ^d	T_o	T_{mid}	T_f	ΔC_p ^e
100% EBU	88	115	12.2	89.6	67	16.6	-45.2	-39	-32.9	0.367
85/15 EBU/PS	82.8	110.9	10.7	73.6	45.6	14.5	-42.2	-37.2	-32.1	0.28
75/25 EBU/PS	96.5	115.4	8.64	88.6	73	9.01	-45.3	-38.8	-32.3	0.257
50/50 EBU/PS	99.8	112.8	6.85	90.1	78.5	5.15	-46.5	-40.6	-34.8	0.174
35/65 EBU/PS	101.9	114.2	4.92	81.8	69.4	3.2	-46.8	-40.8	-34.9	0.13
25/75 EBU/PS	109.7	120.8	0.798	82.8	72.5	1.33	-48.5	-42.5	-36.6	0.092
100% PS	(No melting or crystallization peak)						103.2	107	110.7	0.27

^a All temperatures in °C. Subscripts *o*, *p*, *mid*, and *f* indicate onset, peak, middle, and final temperatures, respectively.

^b Subscripts *m* and *c* indicate melting and crystallization temperatures/enthalpies.

^c T_g indicates glass transition.

^d ΔH is in J/g.

^e ΔC_p is in J/g/°C.

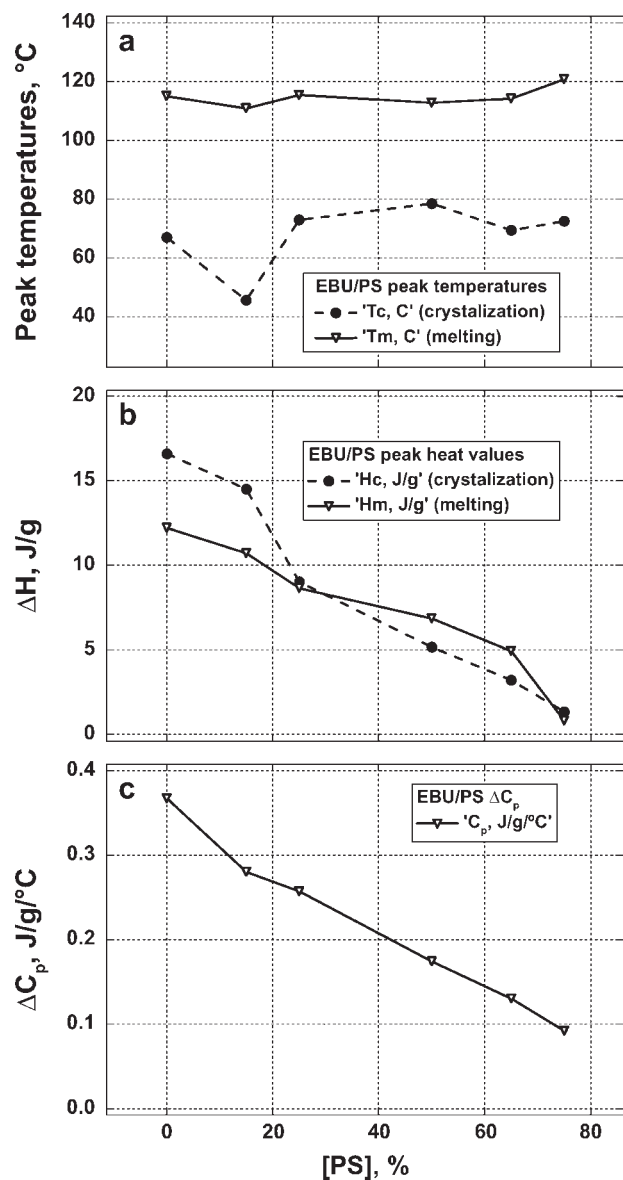


Figure 4 Effect of % PS on (a) melting and crystallization peak temperature and (b) melting and crystallization ΔH , and (c) ΔC_p of EBU/PS bioblends.

are the corresponding heats (ΔH_m , ΔH_c , ΔC_p) for the neat polymers and blends.

The DSC peak of EBU/PS blends at around 110°C could have been either from the T_g of the PS component or from the T_m of the EBU component. As mentioned above, this peak was assigned to be from the T_m of the EBU component. The procedure used to make this assignment was as follows. There are two ways to perform peak assignment when a T_g and an endothermic transition are overlapping in temperature: (1) to re-run the sample for another cycle. The T_g will appear in the re-run and not the transition. During the second cycle one of the polymers in question may crystallize as in our situation, EBU showed an exothermic transition upon cooling,

which makes this method of peak assignment unhelpful. (2) The second method is to use the modulation feature of the DSC as provided by TA Instruments, which is software that can give us a reverse heat information capable of separating the endothermic transition and the T_g , i.e., if a T_g is present but it was masked by the endothermic transition, reverse heating will show only T_g . This feature is one of the practical applications of Modulated DSC developed by TA Instruments. On the basis of this procedure, the peak was assigned to EBU.

Figure 4 compares the effect of blend composition on the peak T_m and T_c values as well as the corresponding heats. As can be seen in Figure 4, with increasing PS concentration in the blend, T_m and T_c displayed slight variation but remained close to the value of neat EBU. However, ΔH_m and ΔH_c decreased with increasing concentration of PS. This is an indication that PS is disrupting the EBU crystalline structure and also preventing EBU from recrystallizing. Figure 4 also shows that ΔC_p decreased with increasing concentration of PS.

Figure 5 shows the effect of PS concentration on T_g of EBU/PS blends. As can be seen in Figure 5, the T_g of the blend was close to the value of neat EBU (-42.5 to -37.2 °C), and showed a slight dependence on PS concentration. The observation is rather unique in that the blend displayed a single T_g

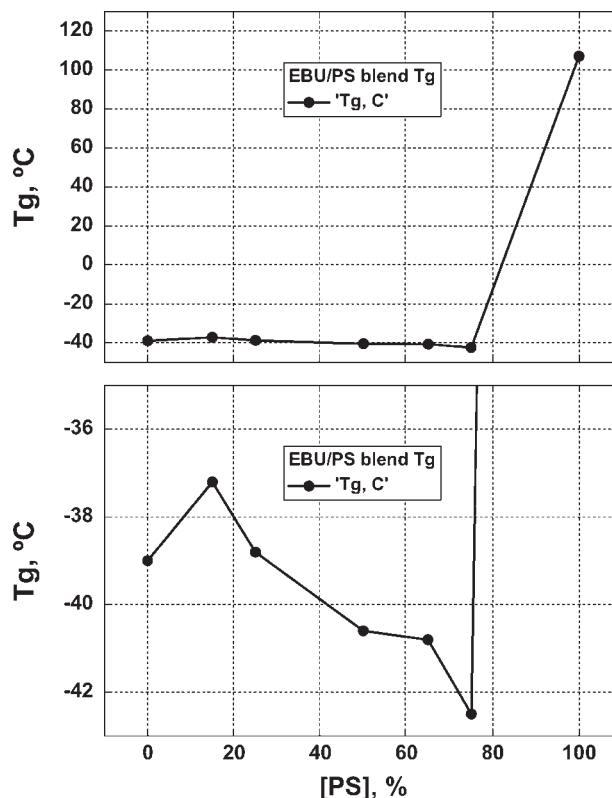


Figure 5 Effect of blend composition on T_g of EBU/PS bioblends.

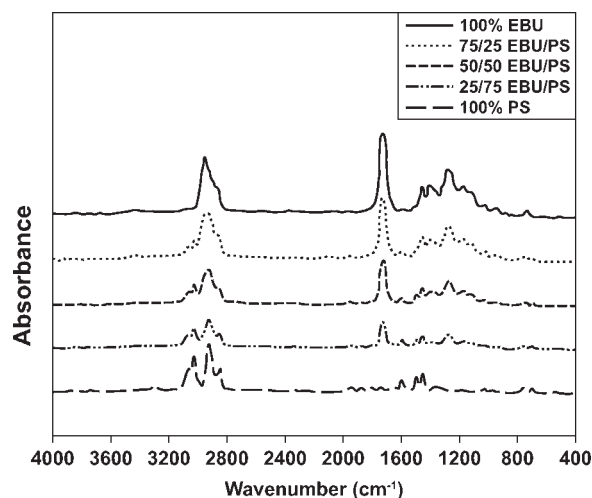


Figure 6 FTIR-PAS spectra of EBU/PS bioblends.

that showed some variation with composition, which is considered an indication of some degree of interaction between the polymers. However, the T_g of the blend did not increase with increasing composition of the polymer with the higher T_g , which in this case is PS. This presents a unique situation where the DSC data does not provide definitive support for the existence or lack of interactions between the polymers. To shed light on this situation, we undertook further investigation of the EBU/PS blend using FTIR-PAS analysis, which is described next.

FTIR-PAS analysis

FTIR-PAS is a nondestructive and nondisruptive method that provides a means to probe the molecular level interactions between the polymers in solid binary blends.^{58–66} It is well suited for analysis of molecular interactions in polymer blends. FTIR-PAS has been originally applied with binary polymer blends.^{67,68}

Figure 6 shows stacked FTIR-PAS spectra of neat EBU, neat PS, and EBU/PS blends. As expected, neat EBU displayed a strong carbonyl peak in the range $1850\text{--}1650\text{ cm}^{-1}$, whereas no such peak was observed for neat PS. Also, as expected, the intensity of the carbonyl peak decreased with increasing concentration of PS in the blend. An interesting aspect of the data in Figure 6 is the fact that a single broad peak was observed for the carbonyl group even though there are two different carbonyl groups in EBU. This is because the EBU polyester comprises two different ester groups: tetramethylene adipate and terephthalate. Visualization of the carbonyl peaks corresponding to each ester group requires further processing of the broad carbonyl peak in Figure 6, following the procedure outlined in the Experimental. By this conventional procedure the EBU/PS

blends were not significantly different. A typical result from such processing (spectrum of neat EBU and 50/50 EBU/PS blend) is shown in Figure 7.

The data in Figure 7 show several interesting features. First, the broad carbonyl peaks for both neat EBU and 50/50 EBU/PS blend shown in Figure 6 have been transformed into their corresponding underlying peaks. Second, the positions of these underlying peaks in the 50/50 EBU/PS blend have been shifted to lower wavenumbers relative to those of neat EBU. The shifts were from 1736 and 1713 cm^{-1} in neat EBU to 1728 and 1709 cm^{-1} , respectively, in EBU/PS 50/50 blend. Such absorbance shift is an indication of weakening of the carbonyl bond due to weakening of the force constant of the C=O bond. One possible explanation for such occurrence is the possible existence of some sort of interaction between the carbonyl group in EBU and the phenyl group in PS as depicted in Figure 8.

Compatibility in EBU/PS blends

In this section, we discuss the implications of the TGA, MDSC, and FTIR-PAS results on blend compatibility. Polymer blend compatibility is a spectrum of properties between two extreme values. On one end of the spectrum are polymer blends that are fully compatible, i.e., fully miscible at all compositions and temperatures. Very few such blends have been identified over the years.²⁴ On the other end of the spectrum are polymer blends that are totally incompatible, i.e., those that completely separate into their respective component domains at all compositions and temperatures. Most polymer blends display compatibility properties that are intermediate between these two extreme values. Such polymer blends are called partially compatible blends, because they display some of the characteristics considered indicators of compatibility.

TGA/DTGA investigation showed that neat EBU is less thermally stable than PS. It also showed that

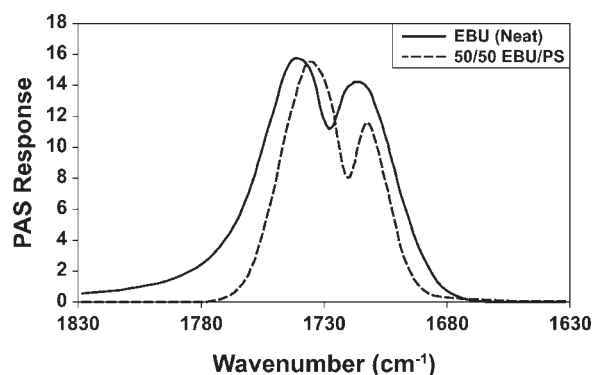


Figure 7 Resolution and visualization of FTIR-PAS carbonyl bands of EBU and 50/50% EBU/PS bioblend.

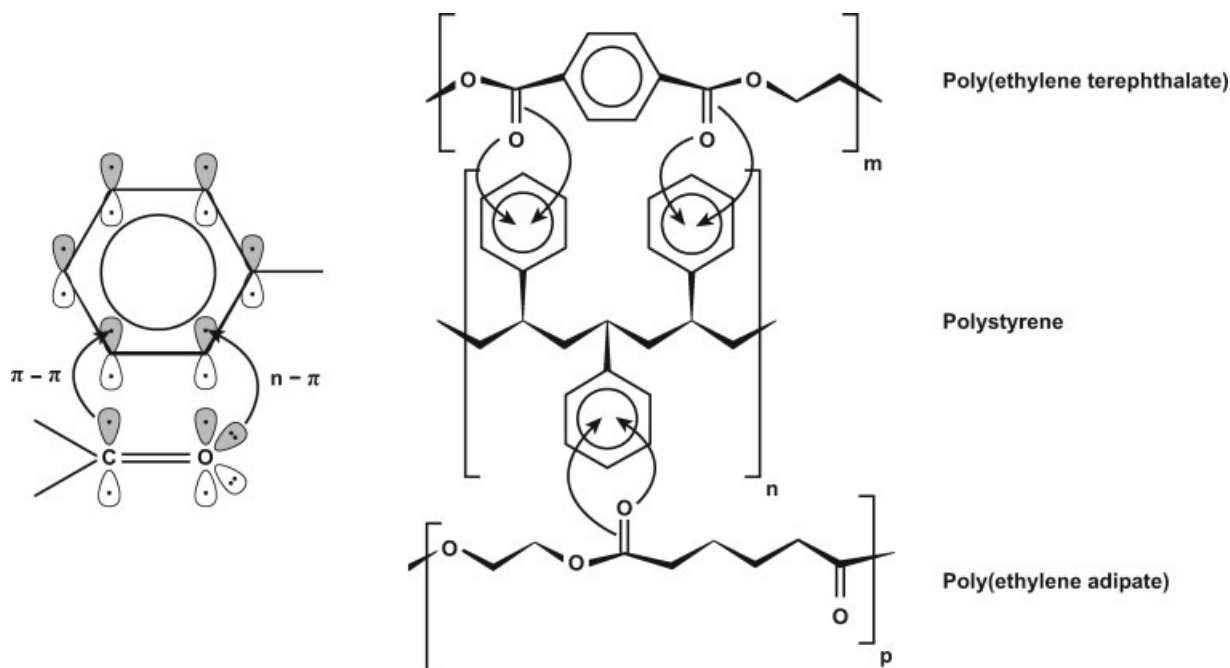


Figure 8 Schematics of proposed n - π and π - π bond complex structure in EBU/PS bioblends.

EBU displayed 6 and 3% char residues at 440 and 800°C, respectively, whereas neat PS displayed no char residue. Three important observations from TGA and DTGA investigation of EBU/PS blends were: (a) blends displayed a simple thermogram with no shoulders at all compositions, (b) blends thermally degraded completely without leaving any char residue, and (c) some blends displayed peak and/or final decomposition temperatures that were higher than those for neat PS, the more thermally stable blend component. These observations seem to indicate that blends are thermally degrading as a homogenous unit as opposed to each component degrading separately. If the later was the case, the thermogram would have displayed a shoulder at the temperature where the second and the more stable component (PS) begins its thermal degradation. In addition, the DTGA data would have displayed multiple peaks as opposed to the single peaks that were observed for all blends. The fact that there were no char residues from the blends might be an indication that PS is acting as a catalyst to bring about complete thermal degradation of EBU. The fact that some blend compositions displayed better thermal stability than PS implies that some sort of interaction between the components resulted in a homogenous complex with improved thermal stability. The overall conclusion from the TGA investigations can be interpreted as supporting the existence of some sort of interaction between EBU and PS polymers leading to partial compatibility in the EBU/PS blends.

DSC and MDSC measurements showed T_g for PS, and T_g and T_m for EBU, whose values were within the range reported by the manufacturers. DSC and MDSC investigations also showed the existence of a single T_g and a single T_m by all the blends. These single T_m and T_g values were in the range of the values for neat EBU, and were also found to be independent of blend composition. The existence of single T_g and T_m that is concentration dependent is one of the indicators of partial compatibility.⁸ Since the observed T_g and T_m values were concentration independent, the criterion for partial compatibility is not met. Thus, the results of the DSC/MDSC investigations of the EBU/PS blends can be considered as inconclusive when it comes to deciding about partial compatibility.

FTIR-PAS investigations showed strong carbonyl absorption peaks for neat EBU and for EBU/PS blends. The intensity of the carbonyl peaks decreased with increasing concentration of PS in the blend. This is a mass effect resulting from the increase in PS with no corresponding increase in contribution from the carbonyl groups. The broad carbonyl peaks were resolved into two underlying peaks corresponding to the two ester groups (terephthalate and tetramethylene adipate) of the EBU copolyester. An important observation of the FTIR-PAS result was the relatively small shifts, 8 cm^{-1} for the adipate and 4 cm^{-1} for the terephthalate carbonyls, respectively, to lower wavenumber for the 50/50 EBU/PS blend relative to those of neat EBU. Frequency shifts are considered to be an indication of

the existence of intermolecular interaction in polymer blends.⁶⁶ These shifts to lower wavenumber might be an indication of the weakening of the carbonyl double bond due to lengthening of C=O bond as a result of intermolecular interaction. For the blend system investigated here, there are two possible intermolecular interactions. The first is n- π interaction,^{42,67,68} i.e., between the lone electron pairs of the carbonyl oxygens of EBU and the π electrons of the phenyl ring of PS. The second is π - π interaction, i.e., between the π electrons of the carbonyl double bonds in EBU and the π electrons of the phenyl ring in PS. Schematics of n- π and π - π interactions with the electron orbital interactions depicted are shown in Figure 8. At this time, we cannot be certain as to which type of interaction is dominant. Regardless, any intermolecular interaction is an indication of partial compatibility. Thus the results of the FTIR-PAS investigation support the existence of partial compatibility in EBU/PS blends.

CONCLUSIONS

On the basis of the current study, the following conclusions are arrived at regarding compatibility in EBU/PS blends.

TGA/DTGA results predict partial compatibility for the following two reasons:

1. Blends displayed a simple, shoulder-free TGA thermogram with a single DTGA peak,
2. Some blends displayed a higher peak and/or final decomposition temperatures than the more thermally stable blend component, PS.

These observations imply that the blend components thermally degraded as a homogeneous unit, but not as separate components following the profiles of the respective neat polymers.

DSC/MDSC results were inconclusive about degree of compatibility, since it showed a single T_m and single T_g that were independent of blend composition. Such results do not meet the criterion for partial compatibility of polymer blends by the method of DSC, which stipulates the existence of concentration-dependent single T_g and single T_m . Since our results do not meet this criterion, the DSC results are declared inconclusive.

FTIR-PAS results support the existence of partial compatibility. The data show that the carbonyl absorption bands shifted slightly to a lower wavenumber in 50/50 EBU/PS blend relative to that in the neat EBU. Such shifts of absorption bands to lower wavenumbers imply a weakening of the carbonyl double bond due to lengthening of carbonyl bond induced by overlap with the aromatic π -system. This can only be achieved if there is some sort

of interaction between the carbonyl groups in EBU and the aromatic electron cloud in PS. We propose n- π and π - π electronic interactions between the carbonyl groups in EBU and the phenyl rings of PS.

On the basis of the TGA and FTIR-PAS results, it can be concluded that there exists some degree of partial compatibility in EBU/PS blends. This is important since the development of useful polymer blends requires some degree of compatibility between blend components. The results from this work provide encouragement for pursuing the development of biomaterials from EBU/PS blends.

It is not clear why the DSC/MDSC investigations provided inconclusive results about compatibility in EBU/PS blends. We are currently trying to understand the inconsistencies between the methods used in this work. We will also explore other methods of probing compatibility in polymer blends to improve our understanding.

The authors thank Jason Adkins for conducting the MDSC and TGA experiments; Gary Grose, Brian Jasberg, Armand Loffredo, Andrew Thomas, and Richard Westhoff for their help with blend extrusion; and McShell (Hairston) Clarke for technical assistance with the FTIR-PAS measurements.

References

1. Mohanty, A. K.; Misra, M.; Hinrichsen, G. *J Macromol Mater Eng* 2000, 276/277, 1.
2. Wang, X. L.; Du, F. G.; Jiao, J.; Meng, Y. Z.; Li, R. K. Y. *J Biomed Mater Res Part B* 2007, 83, 373.
3. Lu, J.; Qiu, Z.; Yang, W. *Polymer* 2007, 48, 4196.
4. Lee, S.; Lee, Y.; Lee, J. W. *Macromol Res* 2007, 15, 44.
5. Al-Saigh, Z. Y. *ACS Symp Ser* 2006, 939 (Degradable Polymers and Materials), 320.
6. Qiu, Z.; Yang, W.; Ikehara, T.; Nishi, T. *Polymer* 2005, 46, 11814.
7. Kalambur, S.; Rizvi, S. S. H. *J Appl Polym Sci* 2005, 96, 1072.
8. Jia, X.; Wang, X.; Tonelli, A. E.; White, J. L. *Macromolecules* 2005, 38, 2775.
9. Huang, H.; Hu, Y.; Zhang, J.; Sato, H.; Zhang, H.; Noda, I.; Ozaki, Y. *J Phys Chem B* 2005, 109, 19175.
10. Guan, J.; Fang, Q.; Hanna, M. A. *J Polym Environ* 2004, 12, 57.
11. Tsuji, H.; Ishizaka, T. *Int J Biol Macromol* 2001, 29, 83.
12. Park, S. H.; Lim, S. T.; Shin, T. K.; Choi, H. J.; Jhon, M. S. *Polymer* 2001, 42, 5737.
13. Li, J.; He, Y.; Inoue, Y. *Polym J (Tokyo, Jpn)* 2001, 33, 336.
14. Canale, P.; Mehta, S.; McCarthy, S. *J Appl Med Polym* 2001, 5, 65.
15. Tudorachi, N.; Cascaval, C. N.; Rusu, M. *J Polym Eng* 2000, 20, 287.
16. Park, J. W.; Im, S. S.; Kim, S. H.; Kim, Y. H. *Polym Eng Sci* 2000, 40, 2539.
17. Meredith, J. C.; Amis, E. *J Macromol Chem Phys* 2000, 201, 733.
18. Mohamed, A. A.; Gordon, S. H. In *Thermal Analysis Applications Conference, Proceedings*; The Adhesion Society: Virginia, 2002; p 281.
19. Shogren, R.L.; Willett, J. L. In *Annual Technical Conference – Society of Plastics Engineers*; North American Thermal Analysis Society: Pennsylvania, 2001; p 1860.
20. Willett, J. L.; Shogren, R. L. *J Polymer* 2002, 43, 5935.
21. Ljungberg, N.; Wesslen, B. *J Polymer* 2003, 44, 7679.

22. Hoffman, G. T.; Soller, E. C.; McNally-Heintzelman, K. M. *J Biomed Sci Instrum* 2002, 38, 3853.
23. Olabisi, O.; Robeson, L. M.; Shaw, M. T. *Polymer-Polymer Miscibility*; Academy Press: New York, 1979.
24. Utracki, L. A. *Polymer Alloys and Blends*; Hansen: New York, 1990.
25. Wu, S. *Polymer Interface and Adhesion*; Dekker: New York, 1982.
26. Paul, D. R.; Bucknall, C. B., Eds. *Polymer Blends Formulation*; Wiley: New York, 2000; Vol. 1.
27. Biresaw, G.; Carriere, C. J. *J Polym Sci B: Polym Phys* 2002, 40, 2248.
28. Biresaw, G.; Carriere, C. J. *J Appl Polym Sci* 2002, 83, 3145.
29. Biresaw, G.; Carriere, C. J. *Prepr ACS Div Polym Chem* 2002, 43, 367.
30. Biresaw, G.; Carriere, C. J.; Willett, J. L. In *26th Annual Meeting of the Adhesion Society, Proceedings*; The Adhesion Society: Virginia, 2003, p 154.
31. Biresaw, G.; Carriere, C. J. *Compos A* 2004, 35, 313.
32. Felker, F. C.; Biresaw, G. *J Biobased Mater Bioenergy* 2007, 1, 401.
33. Anand, J.; Palaniappan, S.; Sathyanarayana, D. N. *J Polym Sci Part A: Polym Chem* 1998, 36, 2291.
34. Vazquez-Torres, H.; Cauich-Rodriguez, J. V.; Cruz-Ramos, C. A. *J Appl Polym Sci* 1993, 50, 777.
35. Ray, I.; Roy, S.; Khastgir, D.; *Polym Bull (Berlin, Ger)* 1993, 30, 685.
36. Goel, M.; Singhal, R.; Nagpal, A. K.; Kandpal, L. D. *Mater Manuf Process* 2001, 16, 427.
37. Liao, G.; Jian, X.; Wang, J. J.; *Mater Sci Technol (Shenyang, China)* 2002, 18, 561.
38. Mehta, A.; Isayev, A. I. *J Polym Eng Sci* 1991, 31, 963.
39. Mi, Y.; Zheng, S.; Chan, C. M.; Guo, Q. *J Appl Polym Sci* 1998, 69, 1923.
40. Dodson, B.; McNeill, I. C. *J Polym Sci Part A: Polym Chem* 1976, 14, 353.
41. Isukada, M.; Freddi, G.; Crighton, J. S. *J Polym Sci Part B: Polym Phys* 1994, 32, 243.
42. Jang, L. W.; Lee, D. C. *J Polymer* 1999, 41, 1749.
43. Mi, Y.; Feng, J.; Chan, C.-M.; Guo, Q. *J Appl Polym Sci* 1997, 65, 295.
44. Mielke, W. *J Polym Eng Sci* 1988, 28, 1077.
45. Vieira, F. T.; Mano, V. *J Cienc Eng* 2001, 10, 18.
46. Zheng, S.; Guo, Q.; Mi, Y. *J Polymer* 2003, 44, 867.
47. Zhong, Z.; Mi, Y. *J Polym Sci Part B: Polym Phys* 1999, 37, 237.
48. Flynn, J. H.; Wall, L. A. *J Polym Lett* 1966, 4, 323.
49. Archondouli, P. S.; Kallitsis, J. K.; Kalfoglou, N. K. *J Appl Polym Sci* 2003, 88, 612.
50. Krupa, I.; Luyt, A. S. *J Polymer* 2001, 42, 7285.
51. Wong, A. C. Y.; Lam, F. *Polym Test* 2002, 21, 691.
52. Urzua, M.; Gargallo, L.; Radic, D. J.; *Macromol Sci Phys B* 2000, 39, 143.
53. Wang, F. Y.; Ma, C. C. M.; Wu, W. J. *J Mater Sci* 2001, 36, 943.
54. Ferreira, B. M. P.; Zavaglia, C. A. C.; Duek, E. A. R. *J Appl Polym Sci* 2002, 86, 2898.
55. Lu, X.; Lim, K. Y.; Lim, F. Y.; Liu, L.; Wong, S. C.; Zhao, J. *Plast Rubber Compos* 2002, 31, 147.
56. Manivannan, A.; Seehra, M. S. *Prepr Pap - Am Chem Soc Div Fuel Chem* 1997, 42, 1028.
57. Rao, B. M.; Rao, P. R.; Sreenivasulu, B. *Polym-Plast Technol Eng* 1999, 38, 311.
58. Urban, M. W.; Craver, C. D., Eds. *Structure-Property Relations in Polymers: Spectroscopy and Performance*; American Chem Society: Washington DC, 1993.
59. Koenig, J. L. *J Adv Polym Sci* 1983, 54, 87.
60. Siesler, H. W.; Holland-Moritz, K. *Infrared and Raman Spectroscopy of Polymers*; Marcel Dekker: New York, 1980.
61. Painter, P. C.; Coleman, M. M.; Koenig, J. L. *The Theory of Vibrational Spectroscopy and its Applications to Polymeric Materials*; Wiley-Interscience: New York, 1982.
62. Drapcho, D. L.; Curbelo, R.; Jiang, E. Y.; Crocombe, R. A.; McCarthy, W. J. *J Appl Spectrosc* 1997, 51, 453.
63. Jones, R. W.; McClelland, J. F. *J Appl Spectrosc* 1996, 50, 1258.
64. Rosencwaig, A.; Gersho, A. *J Appl Phys* 1976, 47, 64.
65. Vidrine, D. W. *J Appl Spectrosc* 1980, 35, 314.
66. Koenig, J. L. *Spectroscopy of Polymers*, 2nd ed.; Elsevier: Amsterdam, 1999.
67. Mohamed, A.; Gordon, S. H.; Biresaw, G. *J Appl Polym Sci* 2007, 106, 1689.
68. Mohamed, A.; Gordon, S. H.; Biresaw, G. *J Polym Degrad Stab* 2007, 92, 1177.